

Oxidation of silicon containing steel

E. J. Song¹, D. W. Suh*¹ and H. K. D. H. Bhadeshia^{1,2}

Steels containing sufficient concentrations of silicon tend to form a low melting temperature oxide called fayalite, which then penetrates both the steel and any other oxide to form a mechanical key. As a consequence, routine descaling operations fail to remove all traces of FeO that remain attached to the final product and oxidise to form a red oxide blemish on the surface. The formation of oxides was investigated both experimentally and by developing a new theory that permits the simultaneous formation of a variety of oxides that compete to establish the final oxide structure. The theory forms the basis for studying the evolution of oxide scales as a function of silicon concentration.

Keywords: Red oxide, Silicon steel, Oxidation theory, Simultaneous transformations

Introduction

There is a blemish that forms on hot rolled steels that are relatively rich in silicon content (~ 1 wt-%), known as 'red oxide'.¹⁻³ It refers to a tenaciously attached film of FeO that has sequentially oxidised into Fe₃O₄ and Fe₂O₃, with the latter being the coloured oxide from which the name derives. The reason why routine descaling operations fail to remove the oxide is that a low melting temperature spinel (fayalite Fe₂SiO₄) forms in silicon rich steels, which in turn forms a eutectic with FeO, and its liquid phase penetrates both the steel and any prior oxide.^{3,4} The resulting convoluted interface with the steel provides a mechanical key that prevents the uniform removal of the oxide.

The oxidation process can be complex. Continuous SiO₂ scale usually forms only in alloys containing >2 wt-%Si.^{5,6} At lower concentrations, a silica formed at the scale/steel interface may ultimately react with FeO to form the spinel.⁷ When oxidised above 1173°C, a eutectic mixture of FeO and fayalite formed below the iron oxides Fe₂O₃, Fe₃O₄ and FeO.^{3,8,9} At lower temperatures, a scale composed of an external FeO layer and an inner FeO–fayalite conglomerate layer, interspersed with discontinuous fayalite bands, forms.^{3,10}

The purpose of the present work is both to characterise experimentally the formation of oxides on experimental steels and to develop a framework that permits the factors influencing the simultaneous formation of competing oxides to be studied quantitatively.

Experimental

The work was performed on an experimental alloy of composition Fe–0.1C–0.94Si–1.54Mn (wt-%). Samples (10 × 7 × 5 mm) were cut and their largest surfaces ground using 2000 grit silicon carbide paper, cleaned

ultrasonically in ethanol and then oxidised in air within an alumina tube furnace at 1000 or 1250°C. After 2 h of exposure, the samples were furnace cooled to room temperature over a period of 6 h to avoid thermal shock. It is assumed here that oxide phase transformations do not occur during this cooling; indeed, no evidence was found in the metallographic studies of such transformations, and rapid cooling is in any event impractical given the need to preserve the oxide layers on the steel surface.

Oxidised samples were observed using scanning electron microscopy and transmission electron microscopy (TEM), together with electron microprobe analysis. Cross-sections showing the oxide/metal interface were cold mounted and coated with gold for examination using scanning microscopy. For transmission microscopy, cross-sectional samples were made using focused ion beam machining. The chemical compositions and elemental distributions were determined using energy dispersive X-ray spectra (EDS) and wavelength dispersive spectroscopy (WDS). X-ray diffraction experiments were conducted using Cu K_α radiation with the beam step scanned at 0.2° min⁻¹.

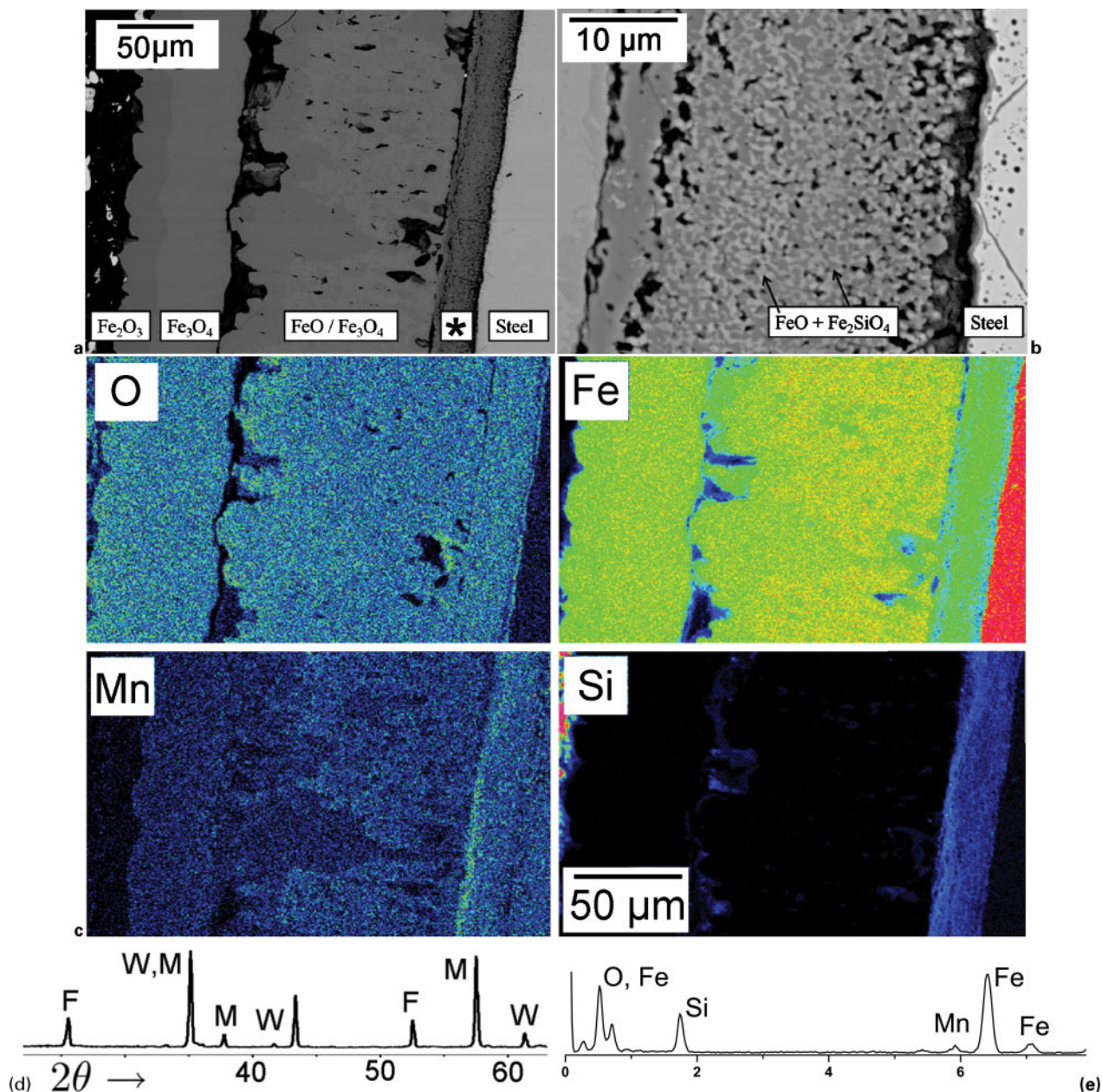
Observations of oxidation

Figure 1 shows that oxidation at 1000°C for 2 h resulted in an oxide composed progressively towards the metal of Fe₂O₃, Fe₃O₄, FeO/Fe₃O₄ and FeO/Fe₂SiO₄ eutectic. The fayalite particle size in the mixture layer was <700 nm, as identified using EDS in TEM. It indicated that the atomic fraction of Fe/Si/O was $\sim 26.5 : 13 : 58.2$. In addition, Mn was detected but it was 2.3 at-%, which could be ignored. Silica (SiO₂) was not observed. The ratio of the outer oxide to that of the mixture FeO/Fe₂SiO₄ was $\sim 88 : 12$, and within the mixture, the ratio of FeO/Fe₂SiO₄ was $\sim 46 : 54$. X-ray diffraction on a sample where the upper layer of oxide was removed confirmed the presence of FeO, Fe₃O₄ and Fe₂SiO₄, as shown in Fig. 1d.

The structure observed is quite different for oxidation at 1250°C for 2 h, where a distinctive eutectic mixture of FeO and Fe₂SiO₄ is evident. This penetrates both into

¹Graduate Institute of Ferrous Technology, POSTECH, Gyungbuk, Korea
²Materials Science and Metallurgy, University of Cambridge, Cambridge, UK

*Corresponding author, email dongwoo1@postech.ac.kr



1 Scanning electron microscope images using atomic number contrast of oxides formed during heat treatment at 1000°C for 2 h. Region marked with asterisk in *a* is presented at higher magnification in *b*. *c* elemental maps. *d* X-ray diffraction; F, W and M stand for fayalite, wüstite and magnetite respectively. *e* TEM EDS result for fayalite

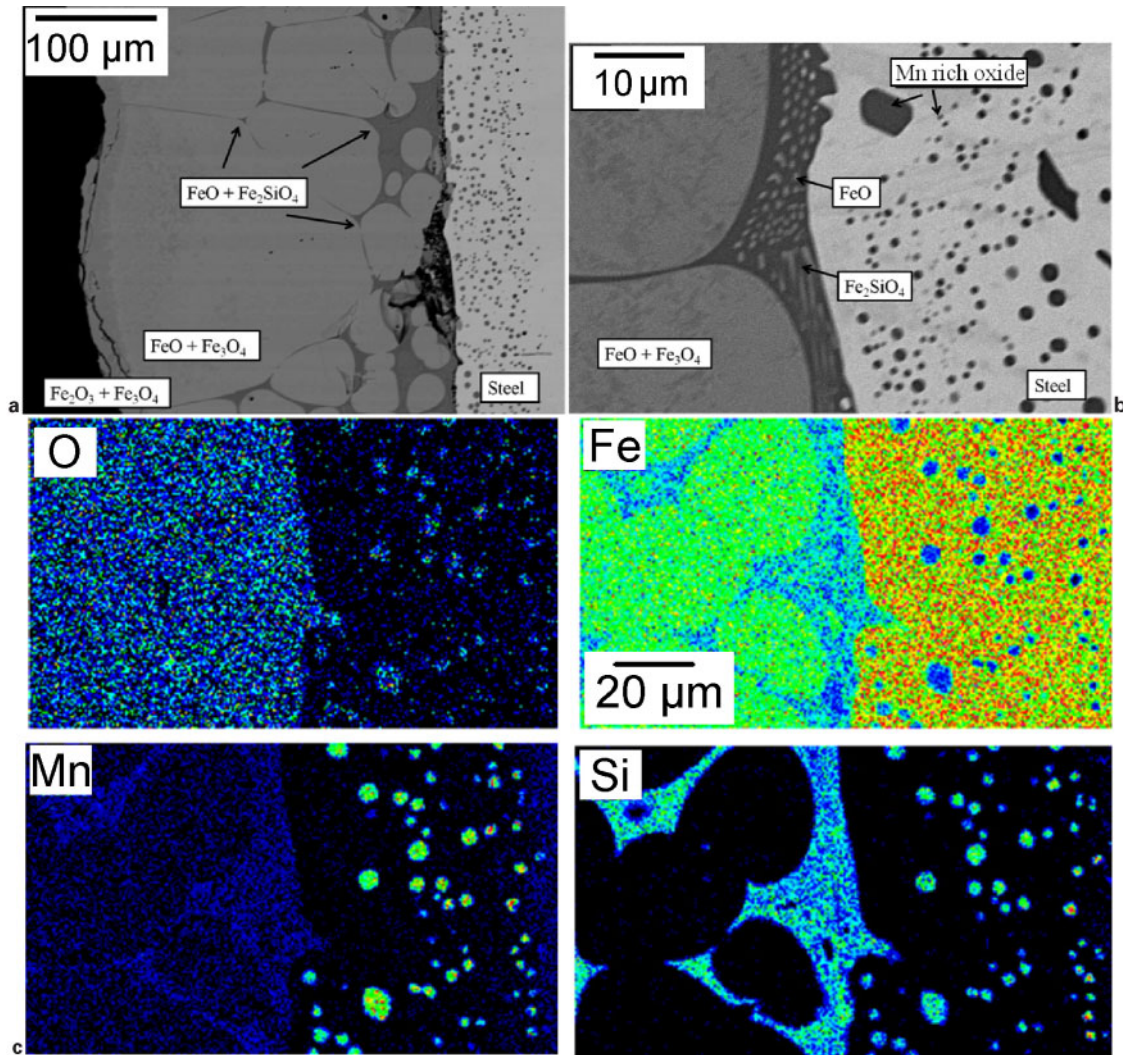
the substrate and along the grain boundaries in the adjacent FeO (Fig. 2). The extent of penetration is much larger within the FeO scale than in the underlying steel; it is speculated that this may have something to do with the wetting ability being greatest when the liquid is in contact with an oxide rather than the metal, and the FeO is of course one component of the eutectic liquid. Manganese rich oxides forming by internal oxidation are seen in the steel beside its interface with the scale, but there is no fayalite present in the steel itself. The eutectic occupied ~15% of the scale, and the ratio of FeO/Fe₂SiO₄ is ~23:77.

Analysis

Figure 3 shows the free energy of formation of a variety of oxides per mole of oxygen in Fe-0.1C (wt-%) steel containing between 1 and 13 wt-% of silicon given a

partial pressure of 0.2 atm of oxygen. The information is from the SUB SGTE database interrogated using MTDATA software.¹¹ The activities of the pure solids were assumed to be 1.0; the reference states for Fe, Si and O₂ were taken to be body centred cubic iron, diamond silicon and gaseous oxygen respectively. It is evident that thermodynamic data alone are insufficient to assess the experimental observations given that silica is the most stable oxide. A phase diagram calculation for Fe-0.1C-0.94Si-1.54Mn (wt-%) steel at 1000°C and $p_{O_2}=0.2$ indicated two oxides in equilibrium with the steel, i.e. ~2 wt-% of silica in the form of tridymite, with the remaining 98% being Fe₂O₃.

It clearly is necessary to deal with the kinetics of oxidation, including the competition between a variety of possible metastable and stable oxides in order to realistically address scale formation. To do this, it is necessary to treat the initiation, growth and impingement



2 a, b scanning electron microscope images using atomic number contrast of oxides formed during heat treatment at 1250°C for 2 h and c elemental maps

of a variety of oxide phases competing to form, so that those with a kinetic advantage become dominant. The thermodynamics of each phase enters implicitly in the theory of diffusion controlled growth via the chemical compositions at the growth interface, which are at local equilibrium.¹²

Growth rate

The oxides were assumed to form on the surface of the steel with the rate controlling step for the formation of silica and fayalite being the diffusion of silicon towards the oxide/metal interface, as illustrated in Fig. 4. The term x^{so} represents the concentration in steel that is in equilibrium with the oxide, and x^{os} is the corresponding value in the oxide that is in equilibrium with the steel. The average concentration of silicon in the steel is \bar{x} . The Zener linearised gradient approximation¹² is used so the diffusion distance is Δz . During isothermal growth over a period t , the rate of oxide thickening is, using standard theory, given by^{12,13}

$$z \frac{dz}{dt} = \frac{D_{Si}(\bar{x} - x^{so})^2}{2(x^{os} - x^{so})(x^{os} - \bar{x})} \tag{1}$$

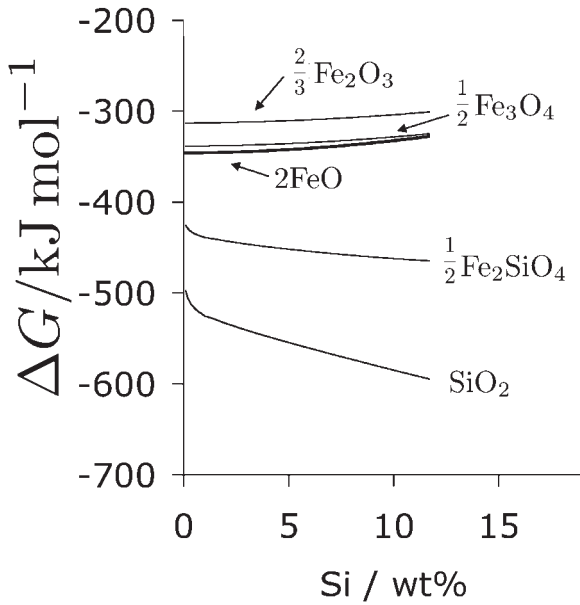
where the term on the right is often written as the parabolic rate constant k in oxidation terminology, and

D_{Si} is the diffusivity of silicon in the austenitic substrate. For both silica and fayalite, the TCFE6 and SSUB4 databases associated with ThermoCalc were used for the equilibrium concentrations, and x^{so} is found to be extremely small at $\sim 10^{-12}$ because of the strong tendency for silicon to oxidise. The concentrations were expressed in atomic fraction, and the values of x^{os} are 0.33 and 0.14 for silica and fayalite respectively. The diffusion coefficients for silicon in austenite and ferrite were obtained from the MOBFE1 database of DICTRA. Figure 5 shows the calculations for the silicon rich oxides during heat treatment at 1000 and 1250°C; the sudden increase in rate beyond 1.9 and 2.8 wt-%Si is a consequence of the change in steel from its austenitic to ferritic state, since the diffusivity of silicon in austenite is relatively slow. Fayalite can form more rapidly than silica because of its smaller silicon concentration, given that the calculations assume that growth is controlled by the diffusion of silicon in steel.

The growth rate of FeO is calculated according to Ref. 14 with

$$k_{FeO} = \frac{1}{2} \int_{P'_{O_2}}^{P''_{O_2}} D_{Fe}^{FeO} d \ln P_{O_2} \tag{2}$$

where FeO is sandwiched between Fe₃O₄, P'_{O_2} is the equilibrium partial pressure of oxygen at the Fe/FeO



3 Oxide formation energy at 1000°C for Fe-0.1C-(1-13)Si (wt-%) steel assuming that partial pressure of oxygen is 0.2 atm

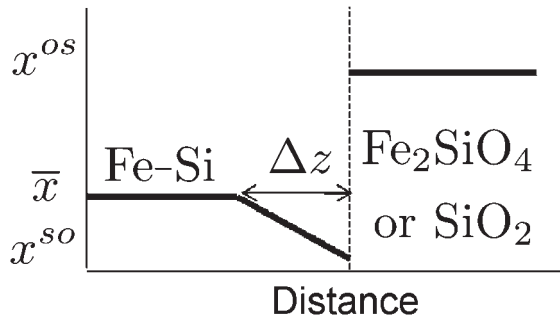
interface and P''_{O_2} is the corresponding value at the FeO/Fe₃O₄ interface. The partial pressures were obtained from the SSUB4 database associated with ThermoCalc. The diffusion coefficient of Fe in FeO was from Ref. 15. The values of k_{FeO} were found to be 0.12 and 6.4 μm² s⁻¹ for 1000 and 1250°C respectively.

Simultaneous oxidation

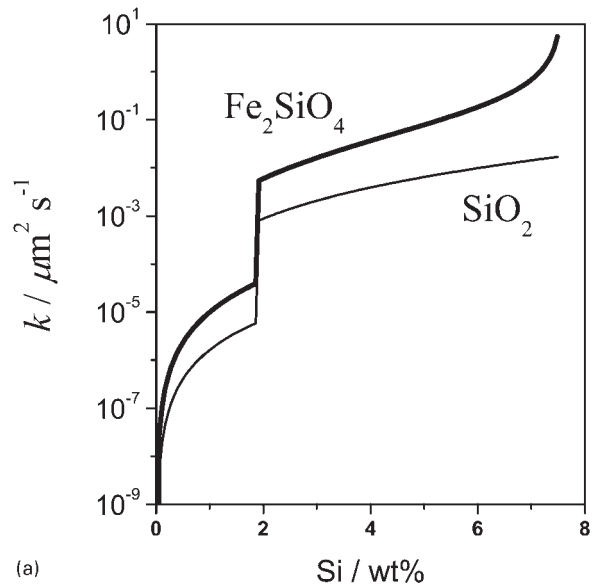
In order to permit the different oxides to form together so that those that have a kinetic advantage dominate, a theory which is a modification of the standard extended volume approach,¹⁶⁻¹⁸ but capable of dealing with many transformations occurring simultaneously,^{19,20} was employed.

Suppose that SiO₂, Fe₂SiO₄ and FeO nucleate on the steel surface and grow both laterally and vertically as hemispherical particles, with vertical growth becoming predominant when the surface is covered completely. We assume additionally that nucleation is unnecessary with growth commencing at time $t=0$ from a specified number of sites. It is possible to calculate an extended area A^c occupied by each oxide, i.e. an area that follows the Avrami procedure¹⁶⁻¹⁸ and in the first instance

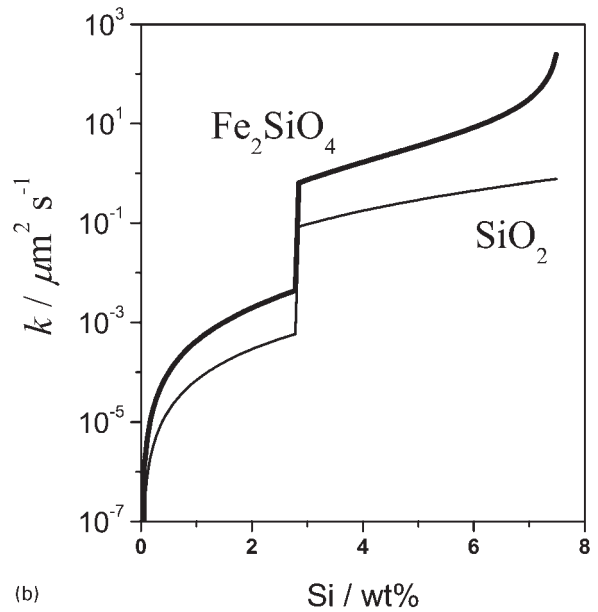
Concentration



4 Distribution of solute Si as function of distance, assuming local equilibrium at oxide/metal interface delineated by dashed vertical line



(a)



(b)

5 Parabolic rate constant k at a 1000°C and b 1250°C as function of silicon concentration

neglects impingement between adjacent particles and allows them to grow through each other. Therefore

$$A_i^c = 2\pi N_i k_i t A_t \tag{3}$$

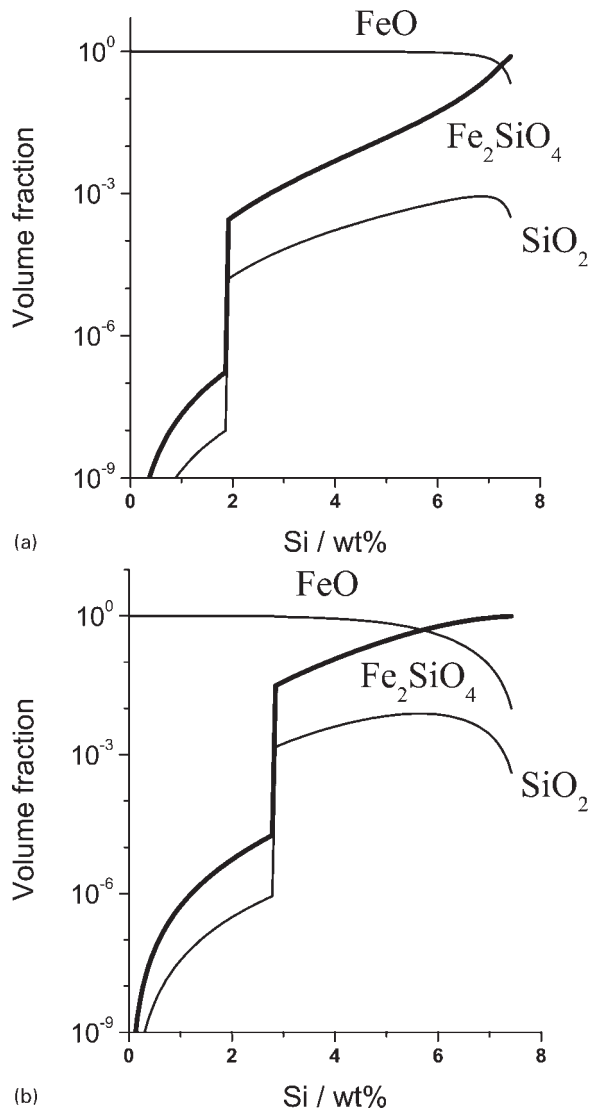
where the subscript i stands for SiO₂, Fe₂SiO₄ or FeO. N represents the number of sites per unit area at which the oxide particles initiate at $t=0$, and A_t is the total steel surface area exposed to oxidation. Any change in extended area (dA^c) coverage can then be converted into a corresponding change in real area (dA) by multiplying with the probability of finding the unoxidised surface

$$dA_i = \left(1 - \frac{A_{SiO_2} + A_{Fe_2SiO_4} + A_{FeO}}{A_t} \right) dA_i^c \tag{4}$$

With the initial condition that there is no oxide at $t=0$, the ratios of areas occupied by each oxide becomes

$$A_{SiO_2}/A_{Fe_2SiO_4}/A_{FeO} = k_{SiO_2} N_{SiO_2} / k_{Fe_2SiO_4} N_{Fe_2SiO_4} / k_{FeO} N_{FeO}$$

Notice that this equation accounts automatically for the distribution of silicon among the oxides. When the



6 Fractions of oxide formed at a 1000°C and b 1250°C at 2 h

surface is fully covered, growth can only occur normal to the surface. The volume (V) occupied by each oxide in the total scale is then given by

$$V_i = A_i(2k_i t)^{1/2} \quad (5)$$

and the volume fractions are in the ratio

$$V_{\text{SiO}_2}/V_{\text{Fe}_2\text{SiO}_4}/V_{\text{FeO}} = (k_{\text{SiO}_2})^{3/2} N_{\text{SiO}_2}/(k_{\text{Fe}_2\text{SiO}_4})^{3/2} N_{\text{Fe}_2\text{SiO}_4}/(k_{\text{FeO}})^{3/2} N_{\text{FeO}}$$

In the absence of information, it is assumed that the number density of initiation sites is identical for each oxide. Figure 6 then shows the evolution of oxides as a function of silicon concentration at both oxidation temperatures. The essential outcome is that FeO, in spite of the lower free energy change associated with its formation, has a huge kinetic advantage because its growth does not require the diffusion of substitutional solute through the steel. From an experimental point of view, the ratio of $V_{\text{SiO}_2}/V_{\text{Fe}_2\text{SiO}_4}/V_{\text{FeO}}$ is 0:6:94 for the 1000°C experiments, which also shows the dominance of the iron oxides.

It is necessary in the future work to include nucleation rates rather than the arbitrarily assumed number densities of initiating particles existing at the beginning of oxidation. To do this would require knowledge of the interfacial energies and number densities of potential sites on the surface where nucleation could occur. Neither of these parameters are known, and unfortunately, it would take a difficult experimental programme to investigate these quantities. It is evident that the model produced here is by no means rigorous, but it does highlight the role of competitive kinetics in determining the constitution of the oxide scale and presents a method that could readily be implemented with greater accuracy if appropriate nucleation functions are discovered.

Conclusions

A model, based on overall transformation kinetics, has been created to estimate the evolution of a mixed oxide scale on the surface of steel containing silicon as an alloying element. The theory is based on simultaneous transformation kinetics that permits more than one oxide to form at the same time, with the detailed phase fractions in the scale depending on the transformation rates.

As a result, and consistent with experimental data, the volume fractions do not scale with thermodynamic stability. It is predicted that even for large silicon concentrations, it is the iron oxides that represent the dominant components of the scale. Although a number of parameters is needed in order to fully implement the kinetic theory, the method may be generalised to include oxides such as alumina in an effort to investigate the prevention of red scale.

Acknowledgements

The authors are grateful for the support from the POSCO Steel Innovation Programme, and to the World Class University Programme of the National Research Foundation of Korea, Ministry of Education, Science and Technology, under project no. R32-2008-000-10147-0.

References

1. T. Fukagawa, H. Okada and Y. Maehara: *ISIJ Int.*, 1994, **34**, 906–911.
2. H. Okada, T. Dukagawa, A. Okamoto, M. Azuma and Y. Matsuda: *ISIJ Int.*, 1995, **35**, 886–891.
3. S. Taniguchi, K. Yamamoto, D. Megumi and T. Shibata: *Mater. Sci. Eng. A*, 2001, **A308**, 250–257.
4. L. Suarez, J. Schneider and Y. Houbaert: *Defect Diffus. Forum*, 2008, **273–276**, 655–660.
5. T. Ban, K. Bohnenkamp and H. J. Engell: *Corros. Sci.*, 1979, **19**, 283–293.
6. A. Atkinson: *Corros. Sci.*, 1982, **22**, 87–102.
7. C. Tuck: *Corros. Sci.*, 1965, **5**, 631–643.
8. L. Suarez, Y. Houbaert, X. V. Eynde and R. Colas: *Corros. Sci.*, 2009, **51**, 309–315.
9. Y. L. Yang, C. H. Yang, S. N. Lin, C. H. Chen and W. T. Tsai: *Mater. Chem. Phys.*, 2008, **112**, 566–571.
10. R. Logani and W. Smeltzer: *Oxid. Met.*, 1969, **1**, 3–21.
11. NPL, MTDATA, Software, National Physical Laboratory, Teddington, UK, 2006.
12. H. K. D. H. Bhadeshia: *Prog. Mater. Sci.*, 1985, **29**, 321–386.
13. J. W. Christian: *Theory of transformations in metal and alloys*, Part II, 3rd edn; 2003, Oxford, Pergamon Press.
14. C. Wagner: 'Atom movements', 153–173; 1951, Materials Park, OH, ASM.

15. W. Chen and N. Peterson: *J. Phys. Chem. Solids*, 1975, **36**, 1097–1103.
16. A. N. Kolmogorov: *Izvestiya Akad. Nauk SSSR (Izvestia Academy of Science, USSR) Ser. Math.*, 1937, **3**, 335–360.
17. M. Avrami: *J. Chem. Phys.*, 1939, **7**, 1103–1112.
18. W. A. Johnson and R. F. Mehl: *TMS-AIMME*, 1939, **135**, 416–458.
19. J. D. Robson and H. K. D. H. Bhadeshia: *Mater. Sci. Technol.*, 1997, **13**, 631–639.
20. S. Jones and H. K. D. H. Bhadeshia: *Acta Mater.*, 1997, **45**, 2911–2920.